

## Activation of p300 Histone Acetyltransferase by Small Molecules Altering Enzyme Structure: Probed by Surface-Enhanced Raman Spectroscopy

K. Mantelingu,<sup>†</sup> A. Hari Kishore,<sup>†,§</sup> K. Balasubramanyam,<sup>†</sup> G. V. Pavan Kumar,<sup>‡</sup> M. Altaf,<sup>†</sup> S Nanjunda Swamy,<sup>§</sup> Ruthrotha Selvi,<sup>†</sup> Chandrima Das,<sup>†</sup> Chandrabhas Narayana,<sup>‡</sup> K. S. Rangappa,<sup>§</sup> and Tapas K. Kundu<sup>\*,†</sup>

Transcription and Disease Laboratory, Molecular Biology and Genetics Unit, Light Scattering Laboratory, Chemistry and Physics of Materials Unit, Jawaharlal Nehru Centre for Advanced Scientific Research, Bangalore-64, India, and Department of Studies in Chemistry, University of Mysore, Manasagangothri, Mysore-06, Karnataka, India

Received: November 17, 2006; In Final Form: February 28, 2007

Reversible acetylation of nucleosomal histones and nonhistone proteins play pivotal roles in the regulation of all the DNA templated phenomenon. Dysfunction of the enzymes involved in the acetylation/deacetylation leads to several diseases. Therefore, these enzymes are the targets for new generation therapeutics. Here, we report the synthesis of trifluoromethyl phenyl benzamides and their effect on histone acetyltransferase (HAT) activity of p300. One of these benzamides, CTPB (*N*-(4-chloro-3-trifluoromethyl-phenyl)-2-ethoxy-6-pentadecyl-benzamide), was discovered as a potent activator of the p300 HAT activity. We have found that pentadecyl hydrocarbon chain of CTPB is required to activate the HAT only under certain context. Furthermore, our results show that the relative position of  $-\text{CF}_3$  and  $-\text{Cl}$  in CTB (*N*-(4-chloro-3-trifluoromethyl-phenyl)-2-ethoxy-benzamide) is also very critical for the activation. Surface-enhanced Raman spectroscopy (SERS) of p300 and the HAT activator complexes evidently suggest that the activation of HAT activity is achieved by the alteration of p300 structure. Therefore, apart from elucidating the chemical basis for small molecule mediated activation of p300, this report also describes, for the first time, Raman spectroscopic analysis of the complexes of histone-modifying enzymes and their modulators, which may be highly useful for therapeutic applications.

### Introduction

A precise organization of chromatin is essential for all DNA templated phenomenon inside the cell. The dynamic alteration of chromatin structure acts as a key regulatory switch in cellular physiology. The post-translational modification of chromatin proteins confers the dynamic nature of chromatin. Specific amino acids within the histone tail and nonhistone proteins are the sites for a variety of modifications, including phosphorylation, acetylation, and methylation.<sup>1,2</sup> Among these, reversible acetylation of histones and nonhistones plays a pivotal role in the regulation of gene expression. Dysfunction of histone acetyltransferases and deacetylases is often associated with manifestation of several diseases including cancer, cardiac hypertrophy, asthma, and diabetes.<sup>3–5</sup> The most widely studied histone acetyltransferases (HATs), CBP (CREB binding protein)/p300, are ubiquitously expressed global transcriptional coactivators, which play crucial roles in different cellular phenomenon including cell cycle control, differentiation, and apoptosis.<sup>6</sup> The transcriptional coactivator function of p300 is at least partially facilitated by its intrinsic HAT activity. Significantly, p300/CBP also acetylates several nonhistone proteins with functional consequences.<sup>7</sup> Mutation in the HAT active site abolishes

transactivation capability of p300/CBP. Analysis of colorectal, gastric, and epithelial cancer samples shows that in several instances, there is a mis-sense mutation as well as deletion mutations in the p300 gene.<sup>8</sup> Mutations in HATs cause several other disorders apart from cancer. Rubinstein-Taybi syndrome has been found to be a result of mutations in CBP. It is interesting that this mutation in CBP also abolishes its HAT activity.<sup>9</sup> The degradation of p300/CBP is also found to be associated with certain neurodegenerative diseases.<sup>10</sup> Hypoacetylated environment could also be created by the hyperactivity or misrecruitment of histone deacetylases. The causal relationship of hypoacetylated histones and manifestation of several cancers is well established. These observations lead to the development of several therapeutic approaches on the basis of histone deacetylase inhibitors.<sup>11,12</sup> The overall nonspecific nature of HDAC (histone deacetylases) inhibitors and its undesired effect on global gene expression inspired us to look for HAT activators. However, very few small molecule modulators of histone acetyltransferases are known so far. Availability of recombinant HATs made it possible to synthesize and also to isolate HAT inhibitors. These include the p300 specific synthetic and natural inhibitor Lysyl CoA<sup>13</sup> and Curcumin,<sup>14</sup> respectively. Recently, we have isolated the first naturally occurring HAT inhibitor anacardic acid from Cashew Nut Shell Liquid and Garcinol from *Garcinia indica*, which are nonspecific inhibitors of p300, CBP, and PCAF (p300/CBP Associated Factor).<sup>15,16</sup> By using anacardic acid as synthon, we have synthesized amide derivative (*N*-(4-chloro-3-trifluoromethyl-phenyl)-2-ethoxy-6-pentadecyl-benzamide) (CTPB), which is the only known small

\* To whom correspondence should be addressed. Phone: 91-80-22082840. Fax: 91-80-22082766. E-mail: tapas@jncasr.ac.in.

<sup>†</sup> Molecular Biology and Genetics Unit, Jawaharlal Nehru Centre for Advanced Scientific Research.

<sup>‡</sup> Chemistry and Physics of Materials Unit, Jawaharlal Nehru Centre for Advanced Scientific Research.

<sup>§</sup> University of Mysore.

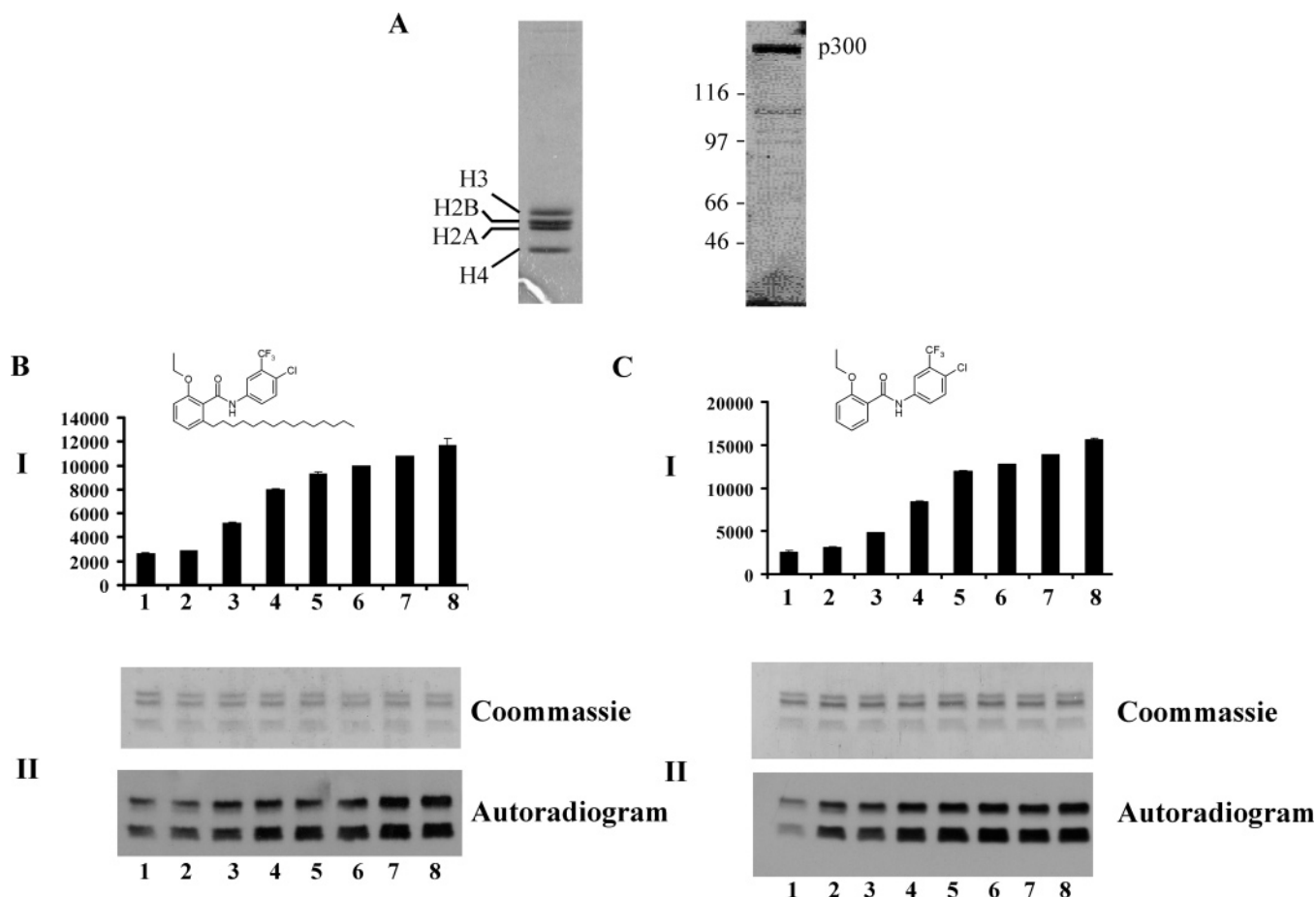


**Figure 1.** (A) Proteins used in different experiments. Highly purified HeLa core histones (2  $\mu$ g) isolated from HeLa nuclear pellet used in the experiment were analyzed by 15% SDS-PAGE (left panel). 800 ng of recombinant His<sub>6</sub>-tagged full-length human p300, purified from baculovirus-infected Sf21 cells and was analyzed by 12% SDS-PAGE (right panel). (B, C) CTPB (**6a**) and CTB (**6j**) enhance p300 HAT activity. Histone acetyltransferase assays were performed in the presence of increasing concentrations of either **6a** (B) or **6j** (C) using HeLa core histones (800 ng) and p300 and were processed for filter-binding assay (panel I). Lane 1, histones with p300; lane 2, histones with DMSO as a control; lanes 3–8, 10, 50, 100, 150, 200, and 250  $\mu$ M of **6a/6j**. The results represent the average values with error bars ( $\pm$ SD) of three independent experiments. Fluorographic analysis of radio-labeled acetylated histones by p300 (panel II). Lane 1, histones with p300; lane 2, histones with DMSO as a control; lanes 3–8, 10, 50, 100, 150, 200, and 250  $\mu$ M of **6a/6j**.

molecule activator of any histone acetyltransferase, in our case p300. Significantly, CTPB is specific to p300 HAT activity. However, the mechanism of CTPB mediated activation of p300 HAT activity is not known. In this report, we have synthesized several derivatives of CTPB and have identified the probable structural basis for the activation of p300 HAT activity. Furthermore, Raman spectroscopic analysis of p300, silver nanoparticle, and different functional derivatives of CTPB complexes suggests that the small molecule activator binding leads to structural changes in the enzyme, which is presumably responsible for the activation of HAT activity.

### Experimental Details

**Materials.** Acetyl coenzyme A [Acetyl-<sup>3</sup>H] (NET-290) was purchased from Perkin-Elmer Life and Analytical Sciences. P81 filter papers used in HAT Filter binding assay were purchased from Whatman (3698-915). Ni-NTA His-Bind resin was purchased from Novagen (70666).

**Purification of Core Histones and Recombinant Proteins.** Histones were purified from HeLa nuclear pellet as described elsewhere.<sup>17</sup> The His<sub>6</sub>-tagged, full-length p300 was purified from the recombinant baculovirus-infected insect cell line, Sf21, through the nickel-nitrilotriacetic acid affinity column (Qiagen) as described previously.<sup>17</sup>

**Histone Acetyltransferase (HAT) Assay.** HAT assays were performed as described previously.<sup>17</sup> Briefly, indicated amounts of core histones were incubated in HAT assay buffer (50 mM Tris-HCl, pH 8.0, 10% (v/v) glycerol, 1 mM DTT, 1 mM PMSF, 0.1 mM EDTA, pH 8.0, 10 mM sodium butyrate) at 30 °C for 10 min in the presence or absence of compound followed by the addition of 0.98  $\mu$ M [<sup>3</sup>H]acetyl-CoA and were further incubated for another 10 min. The final reaction volume was 30  $\mu$ L. The reaction mixture was then blotted onto P81 filter papers, was washed (bicarbonate buffer), and was dried, and radioactive counts were recorded on a Wallac 1409 liquid scintillation counter. For HAT gel assay, the radio-labeled core histones were precipitated using 25% TCA, were resolved on a 15% SDS-PAGE, and were processed for fluorography as described elsewhere.<sup>17</sup>

**Raman Spectroscopy.** The Raman experiments were carried out using the 632.8 nm laser source using the experimental setup described in the earlier work.<sup>18</sup> For the present study, a holographic grating with 1800 grooves mm<sup>-1</sup> was used along with the 200  $\mu$ m spectrograph entrance slit setting, providing  $\sim$ 3 cm<sup>-1</sup> resolution. The laser power used at the sample was 6 mW. To perform surface-enhanced Raman spectroscopy (SERS), we have prepared the citrate-reduced silver colloidal solution following the standard method of Lee and Meisel.<sup>19</sup> We have dissolved 50  $\mu$ L silver colloid to 20  $\mu$ L of p300 solution or a

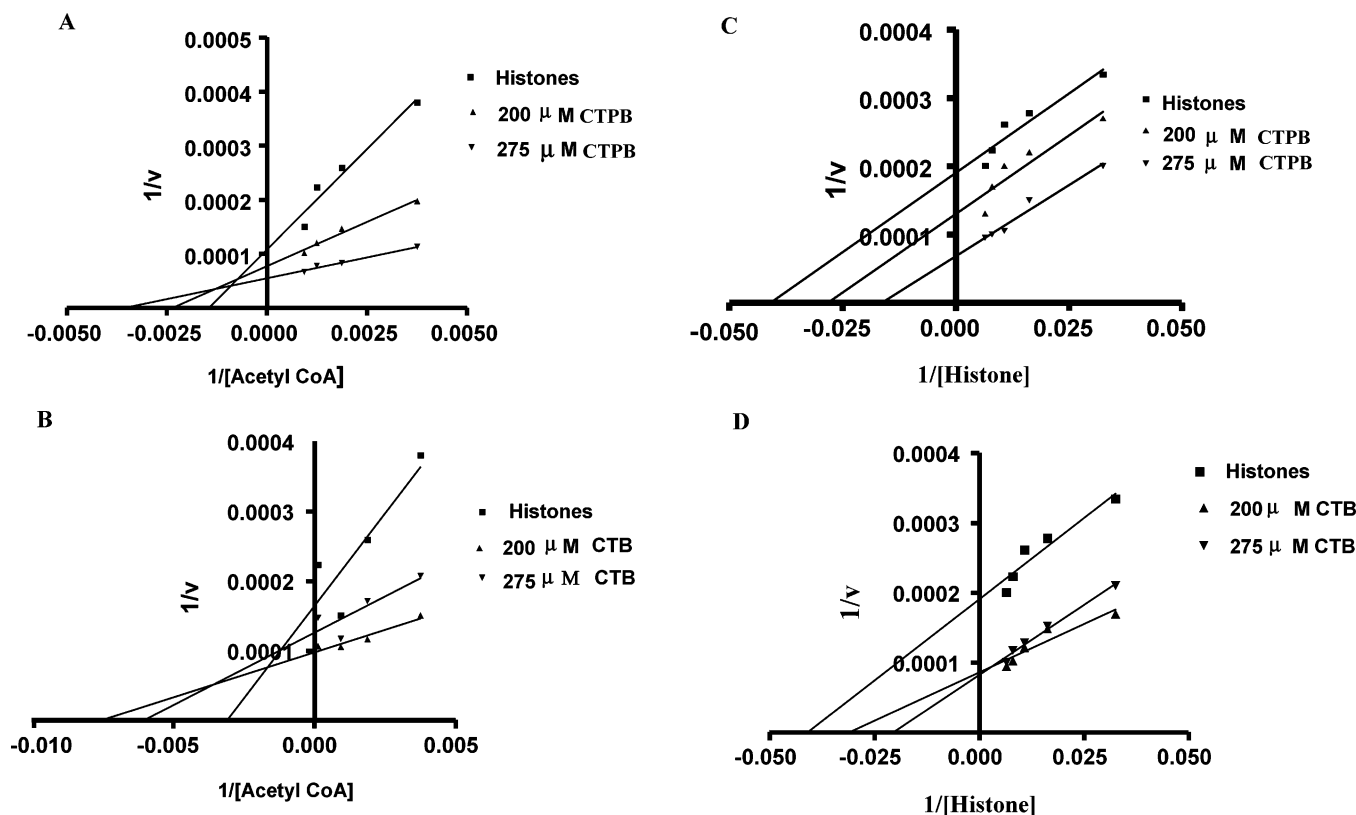


**Figure 2.** Kinetics of p300 HAT activation by CTPB (**6a**) and CTB (**6j**): A and B depict the Lineweaver Burk (LB) plot representation of **6a** and **6j** effect on p300 HAT activity at a fixed concentration of core histones (8 pm) and increasing concentration of [ $^3\text{H}$ ]acetyl-CoA in the presence (200 and 275  $\mu\text{M}$ ) or absence of **6a** and **6j**. C and D show LB plot of the effect on **6a** and **6j** on p300 mediated acetylation of highly purified HeLa core histones (200–275  $\mu\text{M}$ ) at fixed concentration of [ $^3\text{H}$ ]acetyl-CoA (275 nM) and increasing concentrations of histones (0.033–0.165  $\mu\text{M}$ ). The results were plotted using the Graph Pad Prism software.

mixture of 2  $\mu\text{L}$  of CTPB/CTB and 20  $\mu\text{L}$  of p300 solution on a cavity slide under the microscope. The typical accumulation times were 3–5 min. The preincubation time for p300 and compound was kept the same for both Raman experiments as well as enzyme assays.

## Results

### CTPB (**6a**) and CTB (**6j**) Activate p300 HAT Activity.

Recently, we have discovered the first known small molecular activator of histone acetyltransferase p300, CTPB.<sup>15</sup> The structural basis and the mechanism of HAT activation by CTPB were not elucidated. To understand the chemical entities involved in the activation of p300, we have synthesized several derivatives of trifluoromethyl benzamide and have tested their activity using highly purified assay system comprising human core histones from HeLa nuclear pellet and full-length p300 enzyme expressed in the baculovirus infected Sf21 insect cell line (Figure 1A). First, we investigated the role of pentadecyl hydrocarbon side chain of CTPB in the HAT activation. Incubation of p300 with increasing concentration (10–250  $\mu\text{M}$ ) of CTPB (**6a**) resulted in a dose-dependent enhancement of p300 HAT activity ( $\sim 4$  fold at 250  $\mu\text{M}$ ) as estimated by filter-binding HAT assay (Figure 1B, panel I, compare lane 2 vs lanes 3–8). Interestingly, CTB (**6j**), which lacks pentadecyl hydrocarbon chain, also enhanced p300 HAT activity of p300 in a dose-dependent manner similar to CTPB but with a small but consistently higher fold of activation. (addition of 250  $\mu\text{M}$  CTPB showed 10792.37 CPM while CTB showed 13887.17 CPM) (Figure 1C, panel I, compare lane 2 vs lanes 3–8). To visualize the activation of HAT activity by CTPB and CTB, duplicate reactions were subjected to HAT gel fluorography assay. In

agreement with the filter-binding data, the results show that increasing concentrations of the small molecule modulators enhance the HAT activity of p300 (Figure 1B and C, panel II).

We further characterized the nature of activation by enzyme kinetic analysis in the presence of CTPB and CTB. The rates of acetylation reaction at different concentrations of the activators (and its absence) were recorded with increasing concentrations of [ $^3\text{H}$ ]acetyl-CoA and a constant amount of core histones as well as with increasing concentrations of histones and constant amount of [ $^3\text{H}$ ]acetyl-CoA. Lineweaver Burk (double reciprocal) plot of  $1/\text{CPM}$  versus  $1/[\text{^3H}]\text{acetyl-CoA}$  and  $1/[\text{core histones}]$  shows that in the presence of CTPB/CTB,  $K_m$  decreases while  $V_{\text{max}}$  and  $K_{\text{cat}}$  increase with increasing concentration of [ $^3\text{H}$ ]acetyl-CoA and constant amount of core histones (Figure 2A and B). Interestingly, with increasing concentration of core histones and constant amount of [ $^3\text{H}$ ]acetyl-CoA, all the three kinetic parameters  $K_m$ ,  $V_{\text{max}}$ , and  $K_{\text{cat}}$  increased significantly (Figure 2C and D). As observed in the filter-binding assay (Figure 1B and C), kinetic analysis also suggests that at 200  $\mu\text{M}$  and 250  $\mu\text{M}$  concentrations CTB is a better activator of p300 HAT activity as compared to CTPB.

**CTPB (**6a**) and CTB (**6j**) Can Induce Structural Changes in p300.** The kinetic analysis of the activation of p300 activity by CTPB and CTB suggests that in the presence of compounds  $K_m$  is reduced thereby enhancing the enzyme activity. Presumably, binding of the compounds to the enzyme leads to causal change in the enzyme structure to enhance the acetylation activity. We have used a unique approach to monitor the structural change of the enzyme upon binding of the compounds by using SERS. Recently, we have reported the SERS spectrum of p300 and its Raman band assignments.<sup>18</sup> Figure 3 shows the



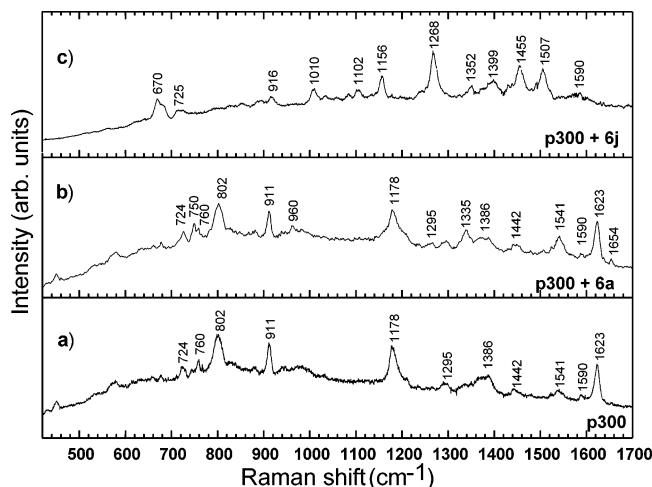


**Figure 3.** SERS spectra of p300 with **6j** (top) and **6a** (middle). (a) Shows the SERS spectrum of p300 and is similar to that reported earlier.<sup>18</sup> Upon addition of CTPB to p300 (b), the SERS spectrum of p300 shows the appearance of certain new modes. In presence of CTB (c), the SERS spectrum of p300 undergoes a large change.

SERS spectra of (a) p300, (b) p300 with CTPB, and (c) p300 with CTB. Whenever a molecule binds to the protein, the binding sites are distanced from the noble metal surface and would make the Raman modes, associated with these regions, reduce in intensity or disappear. The change in orientation of these groups with respect to the nanoparticle surface could also give rise to the disappearance of the Raman mode. SERS is very sensitive to the distance of the metal surface to the molecule as well as the orientation of the molecule itself. Hence, we expect changes in the SERS spectra if the molecule binds to the protein leading to the change in structure, and it gives a clue to the binding sites too. Indeed, in the present case we observe changes in the SERS of p300 in the presence of CTPB and CTB (Figure 3, compare a vs b and c). In the case of CTPB (**6a**) (Figure 3b), the SERS spectrum of p300 does not show large-scale changes. The appearance or increase in intensity of the Raman modes 1654, 1335, and 960  $\text{cm}^{-1}$  suggests that the binding of CTPB is predominantly to the amide groups of the  $\alpha$ -helix and  $\beta$ -sheets.<sup>18</sup> In the case of CTB (**6j**) (Figure 3c), we observe a comparatively larger change in the SERS spectra of p300. This change in the SERS spectra of the protein is rather unusual, but we are confident that the spectrum is indeed of the p300 (see Supporting Information). CTB also binds to the amide groups of the  $\alpha$ -helix and  $\beta$ -sheets like CTPB, but the binding is quite different as we observe disappearance of both 1623  $\text{cm}^{-1}$  and 1654  $\text{cm}^{-1}$  Raman modes. Along with this, the CTB has a strong effect on the binding sites as shown by the large shifts in the peaks in the region 1150–1550  $\text{cm}^{-1}$ , which are related to the amide II and aromatic amino acids (tryptophans (Trp), tyrosines (Tyr), phenylalanines (Phe), and histidines (His)).<sup>18</sup> The shifts in the Raman peaks are between 10 and 35  $\text{cm}^{-1}$ . This is a substantial effect and can be caused only by a strong hydrogen bonding or hydrophobic interaction. The strong interaction of CTB to the amide groups is also reflected in the appearance of a new mode around 1010  $\text{cm}^{-1}$  and 1102  $\text{cm}^{-1}$  (symmetric and asymmetric vibrations of  $\text{C}_\alpha\text{C}-\text{N}$ ) and disappearance of the 802  $\text{cm}^{-1}$  mode (Tyr).<sup>18</sup> The appearance of a mode near 670  $\text{cm}^{-1}$  signifies the interaction of CTB to the carboxyl groups of aliphatic amino acids also. Furthermore, to confirm the observation that the alteration in the SERS spectra upon addition of the activators is indeed generating from the protein p300, SERS of DMSO as well as Ag-nanoparticle has also been done (Supporting Figure 1). These observations

suggest that although both CTPB and CTB bind to p300, affecting the structure of the enzyme, CTB has a greater effect on localized structural alteration (see Discussion). The results show that the DMSO and the Ag-nanoparticle do not contribute in the alteration of p300 SERS spectra. Experiments have also been carried out with varying concentrations of the activator. It is observed that p300 spectra do not change significantly up to 100  $\mu\text{M}$  of CTB. At 100  $\mu\text{M}$  and above, we observe a marked change in the p300 spectra (data not shown).

#### Context-Based Requirement of Pentadecyl Hydrocarbon Chain in CTPB Derivatives to Enhance the HAT Activity.

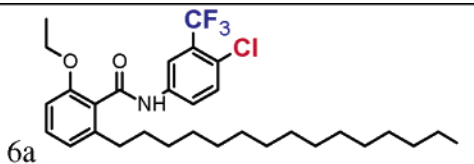
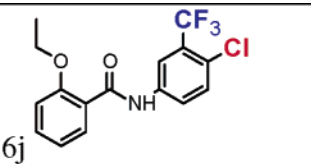
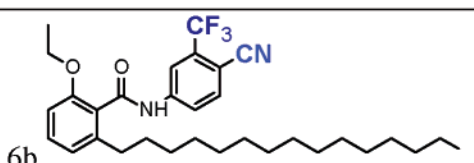
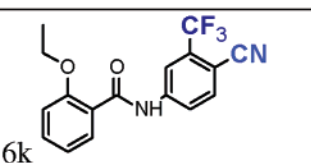
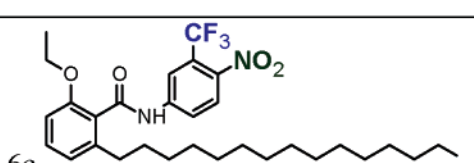
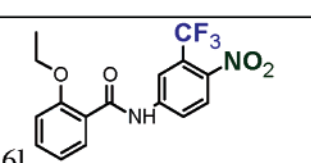
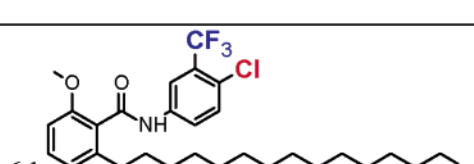
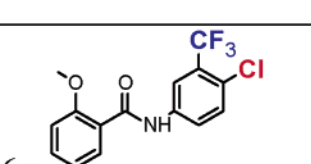
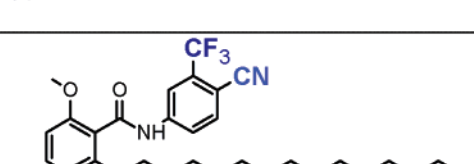
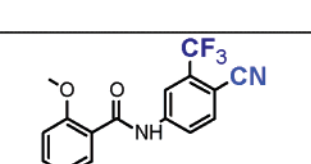
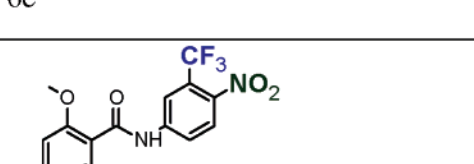
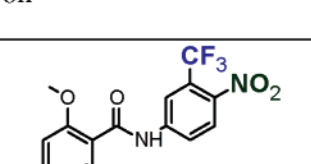
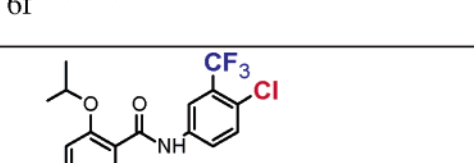
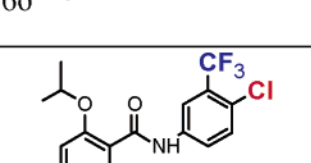
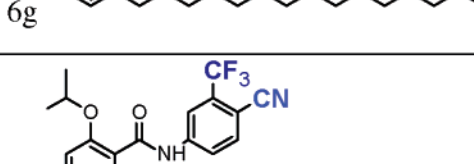
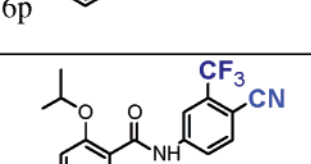
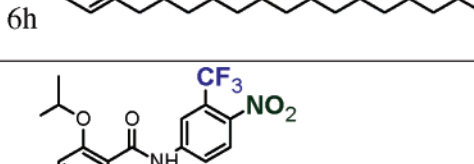
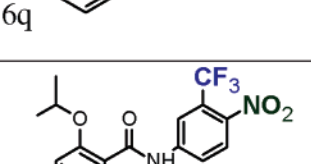
The structural basis of CTPB and CTB to enhance the HAT activity was further investigated using several derivatives of these two classes of compounds. First, several derivatives of CTPB were synthesized keeping the pentadecyl hydrocarbon chain intact, and ethyl and  $-\text{Cl}$  groups were substituted by methyl or isopropyl and  $-\text{NO}_2$  or  $-\text{CN}$  groups, respectively, and were used in HAT assays (Table 1). The results show that all the compounds **6a–6i** could enhance the p300 HAT activity with varying degree at 200  $\mu\text{M}$  concentration. (Table 1 and Figure 4A, compare lane 2 vs lanes 3–11). The results of the filter-binding assay (panel I) were further confirmed by HAT gel fluorography assay (panel II). Surprisingly, we noticed that although CTB derivatives **6p**, **6q**, and **6r** (Figure 4B, lanes 9–11) with isopropyl side chain could enhance p300 HAT activity, the other derivatives (**6m**, **6n**, **6o**, **6k**, **6l**) could not enhance the p300 HAT activity as shown by the filter-binding assay (Table 1 and Figure 4B, compare lane 2 vs 4–8) and HAT gel fluorography assay (Figure 4B, panel II). These results suggest that only isopropyl derivatives of CTB could enhance p300 HAT activity. However, functional analysis of these derivatives could not shed light on the precise requirement of chemical entities required to enhance the p300 mediated histone acetylation.

#### Relative Position of $-\text{CF}_3$ and $-\text{Cl}$ Is Crucial for p300 HAT Activity Enhancement.

To find out the specific positions of functional group required for the enzyme activation, we have synthesized different derivatives of CTB, containing altered positions of  $-\text{CF}_3$  and  $-\text{Cl}$  in the benzamide ring (Figure 5A). The activity of CTB (**6j**), which significantly induces the activity of p300 at 200  $\mu\text{M}$  concentration, was taken as control (Figure 5B lane 3). It was observed that although the *p*-chloro-*o*-trifluoromethyl benzamide (**6s**) and *o*-chloro-*p*-trifluoromethyl benzamide (**6u**) could enhance the HAT activity at 200  $\mu\text{M}$  concentration the fold of activation decreased substantially especially for **6u** (Figure 5B, lane 4 and 6). Most interestingly, we observed that *m*-chloro-*o*-trifluoromethyl benzamide (**6t**) and *o*-chloro-*m*-trifluoromethyl benzamide (**6v**) completely lost the ability to enhance the p300 HAT activity (Figure 5B lane 5 and 7). In agreement with the filter-binding assay, HAT gel fluorographic assay also showed that *m*-trifluoromethyl and *p*-chloro positions are essential for the enzyme activation. These results suggest that the position of  $-\text{CF}_3$  and  $-\text{Cl}$  group is very crucial to induce the activity of p300. After identifying at least partially the chemical basis of the activation of HAT activity, we further investigated, using SERS, whether the activity of the compounds is correlated with the alteration of enzyme structure.

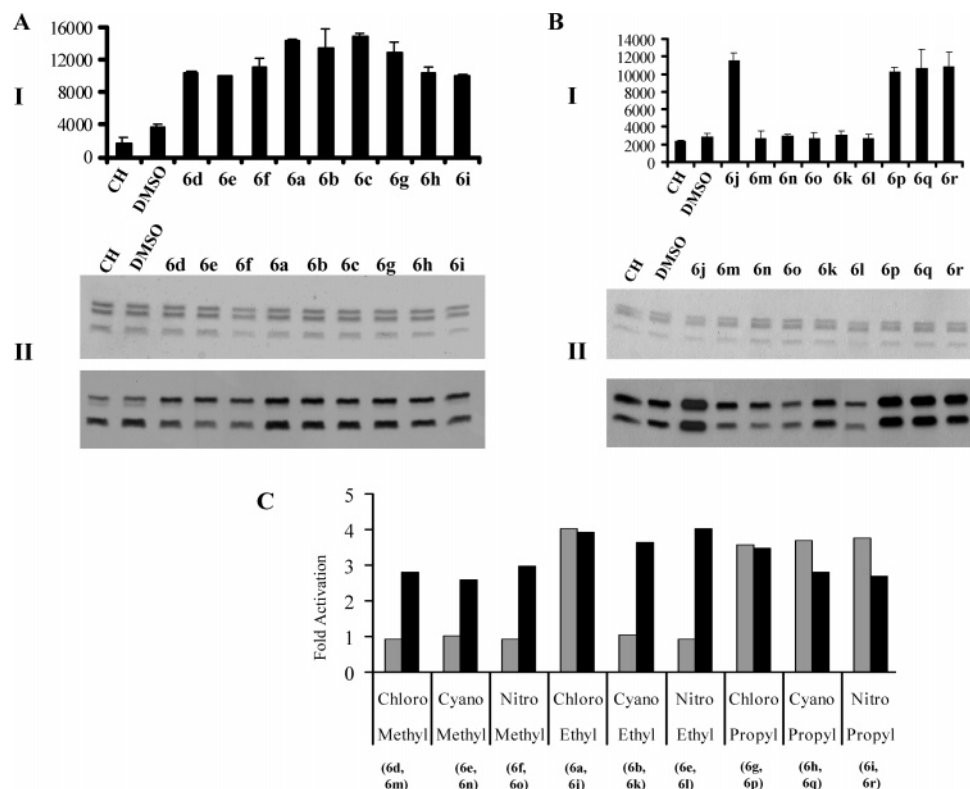
**Compound 6t Failed to Induce Any Change in the p300 Structure.** Figure 6 shows the SERS spectra of p300, in comparison to p300 with **6s**, **6t**, and **6u**. As discussed earlier, the differences in **6s**, **6t**, and **6u** are the relative position of  $-\text{Cl}$  and  $-\text{CF}_3$  on the benzamide ring of **6j**. Interestingly, both **6s** and **6u** induce a large change in the SERS spectra of p300

TABLE 1: Derivatives of Anacardic Acid and Salicylic Acid

 6a	 6j
 6b	 6k
 6c	 6l
 6d	 6m
 6e	 6n
 6f	 6o
 6g	 6p
 6h	 6q
 6i	 6r

(Figure 6, panels b and d). The changes induced by the **6s** molecule is very different from the **6u**, suggesting that both of these molecules interact with the p300 differently, which also

is corroborated in the differential activation of p300 HAT activity (Figure 5B, compare lane 4 vs lane 6). Upon the addition of **6s**, we observe the disappearance of the amide bands around



**Figure 4.** Effect of CTPB (**6a**) and CTB (**6j**) derivatives on p300 HAT activity. Histone acetyltransferase assays were performed in the presence and absence of different derivatives of CTPB and CTB (200  $\mu$ M) using HeLa core histones (800 ng for filter-binding assay and 1600 ng for fluorography) and p300. The samples were processed for filter binding (panel I of A and B for **6a** and **6j**, respectively) or fluorography (panel II of A and B for **6a** and **6j** derivatives, respectively). Lane 1, histones with p300; lane 2, histones with DMSO as a control; lanes 3–11, 200  $\mu$ M of different derivatives. (C) The fold activation of p300 HAT activity by different derivatives of **6j** and **6a** at 200  $\mu$ M concentration.

1623  $\text{cm}^{-1}$  and 1654  $\text{cm}^{-1}$  similar to **6j**. Even **6s**, like **6j**, shows large shifts in the Raman frequencies associated with the amide as well as aromatic amino acid modes (Tyr, Trp, Phe, and His) in the region 1150–1550  $\text{cm}^{-1}$ . The changes in the Raman mode frequencies are around 3–15  $\text{cm}^{-1}$ , except a 35  $\text{cm}^{-1}$  shift in the case of the amide II band around 1541  $\text{cm}^{-1}$ , similar to **6j**. This suggests that the hydrogen bonding and hydrophobic interactions of **6s** are weaker than **6j**, which is also reflected in the difference in their activation of p300 HAT activity. On the other hand, in the case of **6u**, we observe the appearance of strong 1656  $\text{cm}^{-1}$  mode (amide I of  $\beta$ -sheets/random coils) and disappearance of 1623  $\text{cm}^{-1}$  mode (amide I of  $\alpha$ -helix). The amide II band around 1541  $\text{cm}^{-1}$  is shifted by 25  $\text{cm}^{-1}$ . This is much lower than in the case of **6j** and **6s**. The interaction of **6u** to p300 causes shifts in the aromatic amino acid modes (Phe, Tyr, Trp, and His) in the region 1150–1550  $\text{cm}^{-1}$  but to a lesser extent than **6j** and **6s**. The shift in the Raman frequencies again suggests that **6u** induces hydrogen bonding and hydrophobic interaction with p300 around the HAT domain. However, in the case of **6t**, which does not activate the p300 HAT activity, we observe that the p300 spectrum is unaffected or is similar to the pristine p300 (Figure 6c). Taken together, these data suggest that the position of  $-\text{Cl}$  and  $-\text{CF}_3$  has a strong influence in their binding to the p300 and hence the activation of the p300's HAT activity.

## Discussion

Anacardic acid from CNSL (Cashew Nut Shell Liquid) was discovered as the first natural, nonspecific histone acetyltransferase inhibitor.<sup>15</sup> Surprisingly, the amide derivative of anacardic acid was found to specifically enhance the HAT activity of p300. However, the mechanism of activation of the p300 HAT activity

as well as the functional moiety of the compound responsible for the enhancement of activity was not known. Here, we report the synthesis of CTB (**6j**) and the evaluation of the enhancement of p300 HAT activity. We have also synthesized several derivatives of CTPB (**6a–i**) and CTB (**6j–r**). To see whether the long carbon chain in **6a** is responsible for the activation, we synthesized **6j**. Both **6a** and **6j** enhanced the HAT activity of p300. Interestingly, we found that at similar concentrations of **6a** and **6j**, the latter is slightly better activator of p300 (Figure 4). The enzyme kinetic analysis in the presence of compounds **6a** and **6j** shows that  $K_m$  decreases with increasing concentration of [ $^3\text{H}$ ]acetyl-CoA while with increasing concentration of core histones  $K_m$  increases. These data suggest that, presumably, binding of activator to the enzyme alters the enzyme structure in such a way that it recruits more acetyl-CoA which leads to the activation of the enzyme activity. Analyses of the SERS spectra of p300 and the compounds show that indeed binding of the compounds alters the enzyme structure at specific sites (Figures 3 and 6). To confirm the perturbation of backbone conformation of p300 upon compound treatment, we have also performed CD-spectroscopy of p300 and the compound complex. The data showed that although marginal alteration in the CD spectra could be observed in the 220–230 nm range, a dramatic change could be observed in lower wavelength (200–220 nm range). These data suggest that the conformational alteration observed in SERS spectra could be visualized, at least partly by the CD-spectroscopy (Supporting Figure 2). In the wake of the activation data and the kinetics data, the SERS projects a very interesting result, specially related to the changes induced in the structure of p300. Since **6a** and **6j** as well as its derivatives **6s**, **6u**, and **6t** molecules are all hydrophobic in nature, we expect these molecules to form a micellar structure

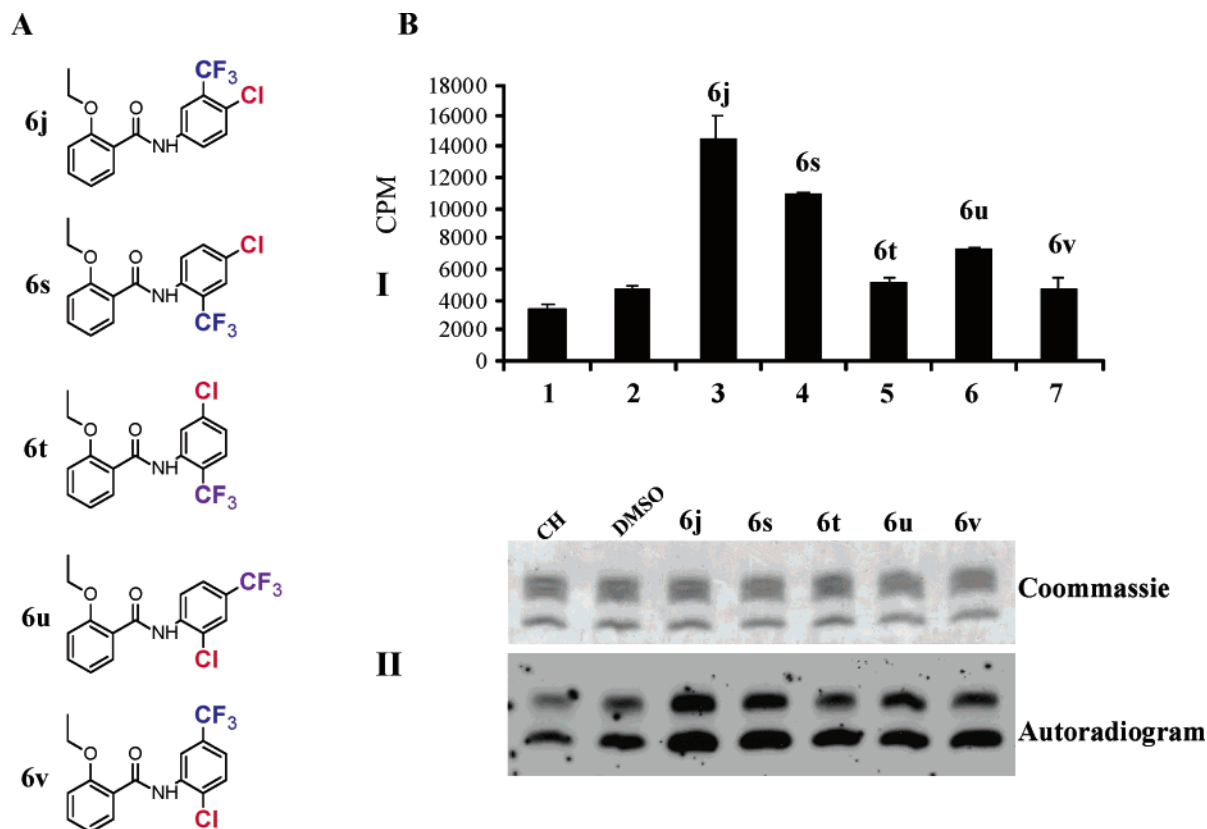


**Figure 5.** Effect of change in the position of  $-\text{CF}_3$  and  $-\text{Cl}$  in **6j** on the HAT activity of p300. Histone acetyltransferase assays were performed in the presence of compounds **6j** and **6(s-v)** (200  $\mu\text{M}$ ) using HeLa core histones (800 ng for filter-binding assay and 1600 ng for fluorography) and p300 and were processed for filter binding (panel I) or fluorography (panel II). Lane 1, histones with p300; lane 2, histones with p300 and DMSO as a control; lanes 3–7, 200  $\mu\text{M}$  of **6j** and **6(s-v)**.

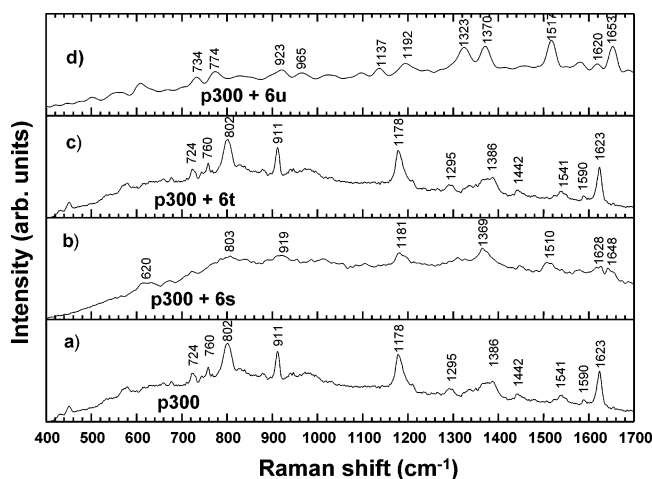


**Figure 6.** SERS spectra of p300 with compounds **6s**, **6t**, and **6u**. The SERS spectrum of p300 is provided in (a) for comparison. In presence of the compound **6s** (b), the SERS spectrum of p300 resembles to some extent Figure 2C. When **6t** is added to p300 (c), the SERS spectrum of p300 resembles that of the curve a. Upon addition of **6u** to p300 (d), the SERS spectrum of p300 again shows a large change but different from the case of **6s** and **6j**.

in aqueous medium and to go into the hydrophobic pockets of the p300 enzyme. Even though these molecules are hydrophobic, they have regions for strong hydrogen bonding as well as hydrophobic interactions. These would be the trigger for the change in the p300 structure. It is well-known that the most hydrophobic region of the p300 is close to the HAT domain of the protein. Hence, the molecules would be causing structural

changes in the HAT domain itself. The basic difference between **6a** and **6j** is the pentadecyl alkyl chain. The long alkyl chain produces a steric hindrance and would put constraint in the effective packing of the micellar arrangement. This is evident in the crystal structure of **6a** and **6j** reported earlier.<sup>15</sup> Presumably, groups, such as  $-\text{CF}_3$ ,  $-\text{Cl}$ ,  $>\text{C}=\text{O}$ ,  $>\text{N}-\text{H}$ , and  $-\text{O}-$  ( $\text{C}_2\text{H}_5$ ), form hydrogen bonding with the p300 and hence affect its structure. The steric hindrance caused by the long alkyl chain of the CTPB reduces the greater chances of hydrogen bonding and hydrophobic interactions in CTPB in comparison to CTB. Probably, this could be the reason for the difference in the change in SERS spectra upon addition of CTPB and CTB. In the case of CTPB, the amide modes are modified, suggesting binding is predominantly hydrogen bonded, which is sufficient enough to activate the HAT function of p300 (see Figure 3a, b).<sup>18</sup> In the case of CTB, in addition to the amide modes, we observe large modifications to the modes associated with ring-structured amino acids like Trp, Tyr, His, and Phe<sup>18</sup> because of both hydrogen bonding and hydrophobic interactions. This added interaction could be the reason for the increase in the activation of the p300 HAT activity in case of CTB. We have found that all molecules **6(a-i)** could enhance the HAT activity, though the degree of activation was not the same. Significantly, in case of **6j** derivatives, only three compounds (**6p**, **6q**, and **6r**) with isopropyl side chain could stimulate the p300 HAT. These results argue for the requirement of pentadecyl hydrocarbon chain under certain context. The physiochemical basis of these data needs further investigation. In search of chemical basis of activation, further we altered the relative position of  $-\text{CF}_3$  and  $-\text{Cl}$  in CTB. Interestingly, we found that the activator effect is



reduced in **6s** and is further reduced in **6u**, while **6t** and **6v** have completely lost the enhancement activity. These results confirm that the relative positions of  $-\text{CF}_3$  and  $-\text{Cl}$  in CTB are important for activation of the protein. It is important to observe that in the case of **6t** there is no functional group in the para position of the phenyl ring of CTB. Addition of **6t** could not alter the SERS spectra of the p300 (Figure 6 panel c), which suggests that the presence of an electronegative group at the para position is responsible for orienting the micellar for stronger interaction with the p300. Both **6s** and **6u** have electronegative groups, namely,  $-\text{Cl}$  and  $-\text{CF}_3$  groups at the para position of the phenyl group of the CTB. The SERS spectra indeed show an increase in the random coils at the expense of  $\alpha$ -helix (compare intensities of 1623, 1295, and  $1654\text{ cm}^{-1}$  in Figure 6a, b, and d) as well as large changes to ring-structured amino acids like Trp, Tyr, His, and Phe<sup>18</sup> in the structure of the p300 upon addition of these compounds. The HAT activity induced by **6s** is relatively low as compared to **6j** but is much larger than **6u**. Therefore, the presence of the  $-\text{CF}_3$  group at the meta position also plays an important role in the activation. It can be inferred that substitution at the meta and para positions in the phenyl group of CTB with strong electronegative group, such as  $-\text{F}$ , may lead to stronger activation of p300 HAT activity. So, in general, the activators of p300 induce changes to the  $\alpha$ -helix and the ring-structured amino acids of the active domain of the protein. This report thus suggests that SERS could be an important tool in the hands of a biochemist to predict the possible compounds which would interact with a protein structure.

## Conclusions

This report describes the identification of chemical entities essential to activate p300 HAT activity by the only known small molecule activator, CTPB. By synthesizing different derivatives of CTPB, we could also elucidate the mechanism of HAT activation. Significantly, by employing surface-enhanced Raman spectroscopy of the enzyme and small molecule compound complexes, we have shown that the activation of HAT activity is achieved by the alteration of p300 structure. Therefore, apart from elucidating the chemical basis, this report also describes for the first time Raman spectroscopic analysis of the complex of histone-modifying enzyme and their modulators, which may be highly useful for therapeutic application as well as to understand the ligand–protein interactions

**Acknowledgment.** We thank Department of Biotechnology, Govt. of India, and Jawaharlal Nehru Centre for Advanced Scientific Research for financial support. R.S. is a CSIR JRF. N.S. is a CSIR SRF. K.M. and A.H.K. contributed equally to this work.

**Supporting Information Available:** The general procedure and scheme for synthesis of the CTPB and CTB derivatives and characterization. Control experiments for SERS and CD spectroscopy of p300. This material is available free of charge via the Internet at <http://pubs.acs.org>.

## References and Notes

- (1) Roth, S. Y.; Denu, J. M.; Allis, C. D. *Annu. Rev. Biochem.* **2001**, 70, 81.
- (2) Shilatifard, A. *Annu. Rev. Biochem.* **2006**, 75, 243.
- (3) Backs, J.; Olson, E. N. *Circ. Res.* **2006**, 98, 15.
- (4) Barnes, P. J.; Adcock, I. M.; Ito, K. *Eur. Respir. J.* **2005**, 25, 552.
- (5) Gray, S. G.; De Meyts, P. *Diabetes Metab. Res. Rev.* **2005**, 21, 416.
- (6) Giordano, A.; Avantaggiati, M. L. *J. Cell. Physiol.* **1999**, 181, 218.
- (7) Dac, C.; Kundu, T. K. *IUBMB Life* **2005**, 57, 137.
- (8) Muraoka, M.; Konishi, M.; Kikuchi-Yanoshita, R.; Tanaka, K.; Shitara, N.; Chong, J. M.; Iwama, T.; Kiyaki, M. *Oncogene* **1996**, 12, 1565.
- (9) Kalkhoven, E.; Roelfsema, J. H.; Teunissen, H.; den Boer, A.; Ariyuerk, Y.; Zantema, A.; Breuning, M. H.; Hennekam, R. C.; Peters, D. *J. Hum. Mol. Genet.* **2003**, 12, 441.
- (10) Cong, S. Y.; Pepers, B. A.; Evert, B. O.; Rubinsztein, D. C.; Ross, R. A.; van Ommen, G. J.; Dorsman, J. C. *Mol. Cell Neurosci.* **2005**, 30, 560.
- (11) Espino, P. S.; Drobic, B.; Dunn, K. L.; Davie, J. R. *J. Cell Biochem.* **2005**, 94, 1088.
- (12) Yeow, W. S.; Ziauddin, M. F.; Maxhimer, J. B.; Shammee-Noori, S.; Baras, A.; Chua, A.; Schrupp, D. S.; Nguyen, D. M. *Br. J. Cancer* **2006**, 94, 1436.
- (13) Lau, O. D.; Kundu, T. K.; Soccio, R. E.; Ait-Si-Ali, S.; Khalil, E. M.; Vassilev, A.; Wolffe, A. P.; Nakatani, Y.; Roeder, R. G.; Cole, P. A. *Mol. Cell* **2000**, 5, 589.
- (14) Balasubramanyam, K.; Varier, R. A.; Altaf, M.; Swaminathan, V.; Siddappa, N. B.; Ranga, U.; Kundu, T. K. *J. Biol. Chem.* **2004**, 279, 51163.
- (15) Balasubramanyam, K.; Swaminathan, V.; Ranganathan, A.; Kundu, T. K. *J. Biol. Chem.* **2003**, 278, 19134.
- (16) Balasubramanyam, K.; Altaf, M.; Varier, R. A.; Swaminathan, V.; Ravindran, A.; Sadhale, P. P.; Kundu, T. K. *J. Biol. Chem.* **2004**, 279, 33716.
- (17) Kundu, T. K.; Wang, Z.; Roeder, R. G. *Mol. Cell Biol.* **1999**, 19, 1605.
- (18) Kumar, G. V. P.; Reddy, A. B. A.; Arif, M.; Kundu, T. K.; Narayana, C. *J. Phys. Chem. B* **2006**, 110, 16787.
- (19) Lee, P. C.; Meisel, D. *J. Phys. Chem.* **1982**, 86, 3391.